

IMAGE INTERPOLATION VIA REGULARIZED LOCAL LINEAR REGRESSION

Xianming Liu¹, Debin Zhao¹, Ruiqin Xiong², Siwei Ma², Wen Gao²

¹School of Computer Science and Technology, Harbin Institute of Technology, Harbin, 150001, China

²Institute of Digital Media, Peking University, Beijing, 100871, China

ABSTRACT

In this paper, we present an efficient image interpolation scheme by using regularized local linear regression (RLLR). On one hand, we introduce a robust estimator of local image structure based on moving least squares, which can efficiently handle the statistical outliers compared with ordinary least squares based methods. On the other hand, motivated by recent progress on manifold based semi-supervised learning, the intrinsic manifold structure is explicitly considered by making use of both measured and unmeasured data points. In particular, the geometric structure of the marginal probability distribution induced by unmeasured samples is incorporated as an additional locality preserving constraint. The optimal model parameters can be obtained with a closed-form solution by solving a convex optimization problem. Experimental results demonstrate that our method outperform the existing methods in both objective and subjective visual quality over a wide range of test images.

Index Terms— Image interpolation, regularized local linear regression, edge preservation.

1. INTRODUCTION

Image interpolation, which addresses the problem of rescaling a low resolution (LR) image to a high resolution (HR) version, is one of the most elementary image processing tasks. Image interpolation has a wide range of applications such as satellite remote sensing, medical analysis and consumer electronics. It is an ill-posed problem by the fact that only a LR version of the original HR image can be observed.

The problem of image interpolation has received much attention from the image processing community. Many image interpolation techniques have been proposed in the literature. The classical data-invariant linear filters, such as bilinear and bicubic [1], have a relatively low complexity, but suffer from the inability to adapt to varying pixel structures which results in blurred edges and annoying artifacts. As well known, the human visual system (HVS), which is the ultimate receiver of the rescaled image, is highly sensitive to distortions of spatial coherence of edges. As a consequence, many researchers advocate the approach of edge-directed interpolation. Li and Orchard [2] propose to match arbitrary edge orientation implicitly by estimating the covariance of HR image from the

covariance of LR image. Zhang and Wu [3] propose to interpolate a missing pixel in multiple directions, and then fuse the directional interpolation results by minimum mean square-error estimation. Directional filtering and estimation have proved to be effective to preserve the edges in image interpolation. Takeda *et al.* propose a novel adaptive generalization of kernel regression with excellent results in image interpolation [4]. Zhang and Wu propose the named SAI algorithm [5], which learns and adapts varying scene structures using a 2-D piecewise AR model, and interpolates the missing pixels in a group by a soft-decision manner. SAI achieves promising results in both objective and subjective performance, and is one of the best performed image interpolation algorithms.

In this paper, we propose an efficient image interpolation technology via regularized local linear regression (RLLR). On one hand, moving weights are incorporated into the objective function to efficiently handle the statistical outliers. On the other hand, we explicitly consider the intrinsic manifold structure by making use of both measured and unmeasured data points and incorporate the geometric structure of the marginal probability distribution induced by unmeasured samples as an additional locality preserving constraint. The major features of RLLR are highlighted as follows: (1) built-in handling of statistical outliers (2) better preserving edge and high frequency features (3) learning with a local linear and global nonlinear manner (4) easy implementation with a closed form solution.

The rest of this paper is organized as follows. Section 2 presents the framework of regularized local linear regression. Section 3 discusses the algorithm details, which include the derivation of transformation vector and the design of spatial weights. Experimental results are presented in Section 4. Section 5 concludes the paper.

2. THE FRAMEWORK OF REGULARIZED LOCAL LINEAR REGRESSION

2.1. Interpolation Model

Supposing $\mathbf{x}_i \in \mathbb{R}^2$ is the pixel to interpolate in the HR image, the problem is how to estimate its intensity y_i with minimum uncertainty from its local neighborhood called training window X . Based on geometric constraint of edges, estimation along the edge orientation is optimal in the sense of best

resolving the uncertainty of y_i . However, edge orientation is hard to precisely describe since it can take any real number. Alternatively, we utilize the strategy of linear weighting of a set candidates $\Phi(\mathbf{x}_i)$, which is the intensity vector of the N nearest neighbors of \mathbf{x}_i from all surrounding directions. Specially, we consider a linear transformation function $f_i(\cdot; \mathbf{a}_i, b_i)$ defined as follows:

$$f_i(\mathbf{x}_i) = \langle \mathbf{a}_i, \Phi(\mathbf{x}_i) \rangle + b_i, \quad (1)$$

where \mathbf{a}_i is a transformation vector; b_i is a translation constant; $f_i(\mathbf{x}_i)$ is the estimated intensity value of \mathbf{x}_i and $\langle \cdot, \cdot \rangle$ is the inner product. One often deals with the bias term b_i by appending each instance with an additional dimension

$$\Phi(\mathbf{x}_i)^T \leftarrow [\Phi(\mathbf{x}_i)^T, 1], \mathbf{w}_i^T \leftarrow [\mathbf{a}_i^T, b_i], \quad (2)$$

then the linear transformation function becomes

$$f_i(\mathbf{x}_i) = \langle \mathbf{w}_i, \Phi(\mathbf{x}_i) \rangle. \quad (3)$$

In the training window X , there are two kinds of points: measured examples (from LR image) and unmeasured ones (from HR image to be interpolated). Our goal is to solve the optimal transformation vector \mathbf{w}_i using the measured and unmeasured information contained in X . Since the function f_i indexed i is defined for each point but not shared by all data points in the training window globally, we refer to it as *local linear regression*.

2.2. Regularized Local Linear Regression

In order to generate high quality HR images, in image interpolation, homogeneous regions should be represented as smoothly as possible, while heterogeneous regions should be as separably as possible. The previous ordinary least squares (OLS) based methods, such as NEDI and SAI, consider all samples in the training window with equal importance, even in the situation where the local neighborhood is on the boundary of two regions. The regions on either side of the boundary may be well approximated with one interpolation model, respectively. However, the regions can be so different that their union cannot be accurately described using the same model, which results in compromise between the two regions. Therefore the edge will be smoothed and do not appear as sharp as they should.

To deal with these multi-model situations, instead of using the OLS based estimation procedure, we exploit a robust estimation technique based on moving least squares (MLS). A robust estimator will only consider the data points from one of the regions and disregard the samples from the other region as being statistical outliers, which is achieved by incorporating moving weights into the objective function to express the relative importance of samples in estimating model parameters.

Let us try to view the image interpolation problem under the framework of regularized local linear regression. Suppose

we are given a training window $X = \{\mathbf{x}_1, \dots, \mathbf{x}_l, \mathbf{x}_{l+1}, \dots, \mathbf{x}_{l+u}\}$. The training data points $X_l = \{\mathbf{x}_j\}_{j=1}^{j=l}$ from LR image serve as measured examples and their intensity values are $Y_l = \{y_j\}_{j=1}^{j=l}$. The rest points $X_u = \{\mathbf{x}_j\}_{j=l+1}^{j=l+u}$ are unmeasured samples to be interpolated. Without loss of generality, we assume \mathbf{x}_i is the current point to interpolate. The optimal transformation vector \mathbf{w}_i is found by projecting the transformation function f_i onto the neighboring measured examples. Given a set of measured examples (\mathbf{x}_j, y_j) , $j = 1, \dots, l$, the local linear regression estimates \mathbf{w}_i by minimizing

$$J(\mathbf{w}_i) = \sum_{j=1}^l \theta(\mathbf{x}_i, \mathbf{x}_j) \|y_j - \mathbf{w}_i^T \Phi(\mathbf{x}_j)\|^2 + \lambda \|\mathbf{w}_i\|^2, \quad (4)$$

where the penalty term is the Tikhonov regularizer [6], which helps to improve the generalization of the solutions. θ is the aperture function, which defines the moving weight reflecting the similarity between \mathbf{x}_i and \mathbf{x}_j . Moving weights are incorporated in the loss function in order to express the relative importance of samples in estimating the parameters of the transformation function. In NEDI and SAI, all points in the local neighborhood are considered equally important, therefore edges may be smoothed and do not appear as sharp as they should.

Motivated by recent progress on manifold based semi-supervise learning [6], we refine the MLS interpolation framework by exploring additional discrimination information hiding in unmeasured samples. From a geometric perspective, there is a probability distribution P on $\mathbb{R}^2 \times \mathbb{R}$ in HR image. The available LR examples are (\mathbf{x}, y) pairs generated according to P , the rest missing examples are simply $\mathbf{x} \in \mathbb{R}^2$ drawn according to the marginal distribution P_X of P . In previous subsection, the induced loss function only expresses relationships between the current unmeasured sample and its neighboring measured examples. By assuming that the support of P_X is a compact manifold, it is more reasonable to incorporate the geometric structure of the marginal distribution P_X induced by unmeasured samples into the image interpolation framework. As such, we proceed to incorporate such knowledge in the loss function through an additional graph-Laplacian prior penalty.

Given measured examples and unmeasured ones in the local neighborhood, we consider the following loss function:

$$J(\mathbf{w}_i) = \sum_{j=1}^l \theta(\mathbf{x}_i, \mathbf{x}_j) \|y_j - \mathbf{w}_i^T \Phi(\mathbf{x}_j)\|^2 + \lambda \|\mathbf{w}_i\|^2 + \eta \sum_{p=l+1}^{l+u} \sum_{q=l+1}^{l+u} \theta(\mathbf{x}_p, \mathbf{x}_q) \|\mathbf{w}_p^T \Phi(\mathbf{x}_p) - \mathbf{w}_q^T \Phi(\mathbf{x}_q)\|^2, \quad (5)$$

where the additional regularization term is the Laplacian penalty, which restricts the intrinsic geometric information of the marginal distribution P_X . The parameters $\lambda > 0$ and

$\eta > 0$ control the relative contribution of two regularization terms in the objective function. As a result, the task of transformation function learning is to minimize the above cost function:

$$\mathbf{w}_i^* = \arg \min J(\mathbf{w}_i). \quad (6)$$

3. ALGORITHM DETAILS

The RLLR algorithm interpolates the unmeasured pixels in the HR image in two pass in a coarse to fine progression. The process of the two passes is illustrated in Fig. 1, in which the black dots are the LR image pixels (measured data) and the rest are the HR image pixels to interpolate (unmeasured data). The first pass is to interpolate the pixels located on the cross, which are regarded as measured points in the second pass. The remaining unmeasured points are to be interpolated in the second pass. In the following, let us consider two key issues in our model: the derivation of transformation vector w and the design of aperture function θ .

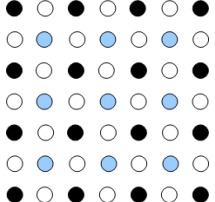


Fig. 1. Interpolation is done in two pass. The first pass is to interpolate the unmeasured points marked by blue circles, and the second pass is to interpolate the remaining unmeasured points marked by white circles.

3.1. Derivation of transformation vector

In practical experiments, for the additional Laplacian penalty, we do not exploit all unmeasured examples but only a subset $\{\mathbf{x}_p\}_{p=l+1}^{p=i-1}$ which have been already interpolated before \mathbf{x}_i with the estimated intensity values $\{\hat{y}_p\}_{p=l+1}^{p=i-1}$. The loss function J can be rewritten as

$$J(\mathbf{w}_i) = \sum_{j=1}^l \theta(\mathbf{x}_i, \mathbf{x}_j) \|y_j - \mathbf{w}_i^T \Phi(\mathbf{x}_j)\|^2 + \lambda \mathbf{w}_i^T \mathbf{w}_i + \eta \sum_{p=l+1}^{i-1} \theta(\mathbf{x}_i, \mathbf{x}_p) \|\mathbf{w}_i^T \Phi(\mathbf{x}_i) - \hat{y}_p\|^2. \quad (7)$$

In order to derive the optimal transformation vector \mathbf{w}_i , we take the derivative of the loss function J in Eq.(7) with respect to \mathbf{w}_i and set the derivative to 0, the optimal \mathbf{w}_i can be represented by

$$\mathbf{w}_i^T = \left(\sum_{j=1}^l \theta_{ij} y_j \Phi(\mathbf{x}_j)^T + \eta \sum_{p=l+1}^{i-1} \theta_{ip} \hat{y}_p \Phi(\mathbf{x}_i)^T \right) \left(\sum_{j=1}^l \theta_{ij} \Phi(\mathbf{x}_j) \Phi(\mathbf{x}_j)^T + \lambda \mathbf{I} + \eta \sum_{p=l+1}^{i-1} \theta_{ip} \Phi(\mathbf{x}_i) \Phi(\mathbf{x}_i)^T \right)^{-1}, \quad (8)$$

Table 1. Objective quality comparison of four interpolation algorithms(in dB).

Image	Bicubic	NEDI	FDI	KR	SAI	RLLR
Airplane	30.17	28.74	30.53	29.11	30.72	30.96
Girl	31.54	31.95	31.81	31.92	31.77	32.24
Peppers	31.59	29.32	31.87	31.02	31.84	32.14
Flowers	25.44	25.70	25.74	25.79	25.96	26.19
Baboon	19.76	20.02	19.87	19.99	19.92	20.32
Door	32.23	32.22	32.27	32.20	32.46	32.60
Butterfly	29.34	28.91	29.67	29.54	29.93	30.31
Tower	39.84	39.85	39.69	40.28	41.49	42.14
Average	30.22	29.59	30.40	29.96	30.75	31.08

where \mathbf{I} is the identity matrix, and we set $\Phi(x)$ as the four nearest neighboring measured examples of x in our experiments.

3.2. The Design of Aperture Function

In the proposed RLLR framework, moving weights provide the prior with the flexibility to model explicitly the local salient features of an image. When local characteristics of the image differ significantly across spatial domain, setting these control weights in regression can efficiently cancel the statistical outliers.

Some efforts in other image processing tasks have been initiated in this direction to determine the similarity of local pattern for better spatial adaptation. *bilateral filter* [7] is proposed to combine gray levels based on both their geometric closeness and their photometric similarity. However, the comparison of the grey level or color values at a single pixel is no more robust when these values get noisier. This drawback is overcome by the *non-local-means* algorithm [8], in which each weight is proportional to the similarity between the local neighborhood of the pixel being processed and the neighborhood corresponding to the other image pixels.

Image priors in product form are very attractive since they have the ability to enforce simultaneously many properties on an image. In this paper, we combine the edge-preserving property of bilateral filter and the robust property of non-local-means weight to design efficient moving weights in regression, which are called patch-based bilateral moving weights as define in Eq. (9).

$$\theta(\mathbf{x}, \mathbf{x}') = \frac{1}{C_{\mathbf{x}}} \exp \left(-\frac{\|\mathbf{x} - \mathbf{x}'\|_2^2}{\sigma_s^2} \right) \exp \left(-\frac{G \cdot \|SW(\mathbf{x}) - SW(\mathbf{x}')\|_2^2}{\sigma_f^2} \right) \quad (9)$$

where G is a Gaussian kernel used to take into account the distance between the central pixel and other pixels in the patch, and $SW(\mathbf{x})$ represents the similarity window which is the neighborhood centered on \mathbf{x} .



Fig. 2. Eight sample images in the test set.

4. EXPERIMENTAL RESULTS AND ANALYSIS

In this section, extensive experiments results are presented to evaluate the proposed new image interpolation scheme in comparison with some representative work in the literature. For thoroughness and fairness of our comparison study, we selected a large set of test images, Fig. 2 lists eight example images in our experiments. The comparison group includes five other image interpolation methods: bicubic interpolation [1], NEDI [2], fused direction interpolation (FDI) [3], kernel regression (KR) [4] and SAI [5].

Table 1 tabulates the objective quality comparison with respect to PSNR of the six different methods. It is clearly seen that for all instances the proposed RLLR algorithm consistently works better than other five methods. Compared with kernel regression interpolation, our method exploits more efficient moving weights and incorporates two regularization terms to keep solution stable and preserve local structure. Therefore, our method can improve 1.12dB in terms of average PSNR. NEDI and SAI are both based on OLS, in which all samples are with the same importance in regression. Our method shows to be quite effective, due to the fact that moving weights are incorporated in the interpolation process to cancel the influence of statistical outliers and the locality preserving constraint can efficiently improve the quality of reconstruction HR images. The RLLR method can improve 1.49dB and 0.33dB with respect to average PSNR compared with NEDI and SAI, respectively.

We also give the subjective quality and interpolation error comparison on wing part of the test image *Butterfly*. As illustrated in Fig. 3, It can be easily observed the RLLR algorithm produces smaller interpolation error than other methods. Such results clearly demonstrate the superiority of the proposed RLLR method in reconstructing the high frequency, such as edges and textures.

5. CONCLUSION

In this paper, we presented a novel image interpolation scheme based on a regularized local linear regression model. Starting with the linear regression model where we replace the ordinary least squares error norm with the moving least squares error norm leads to a robust estimator of local image structure. Moreover, our framework incorporates the geometric structure of the marginal probability distribution induced by unmeasured samples as an additional locality preserving

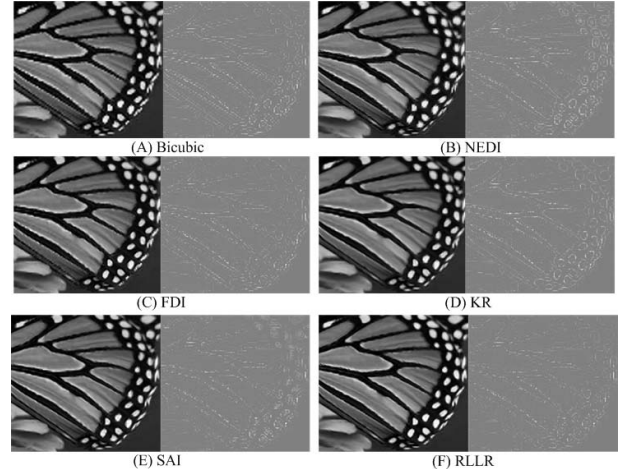


Fig. 3. Subjective quality and reconstruction error comparison for wing part of *Butterfly*. The left are reconstructed HR images, the right are reconstruction errors.

constraint. Experimental results on benchmark test images demonstrate that the proposed method achieves very competitive interpolation performance with the state-of-the-art interpolation algorithms.

6. ACKNOWLEDGMENTS

This work was supported in part by National Science Foundation 60736043 and 61073083, and National Basic Research Program of China (973 Program, 2009CB320905, 2009CB320904).

7. REFERENCES

- [1] R. G. Keys, "Cubic convolution interpolation for digital image processing," *IEEE Trans. Acoust., Speech, Signal Process.*, vol. ASSP-29,no. 6, pp. 1153-1160, Dec. 1981.
- [2] X. Li and M. T. Orchard, "New edge-directed interpolation," *IEEE Trans. Image Process.*, vol.10, no.10, pp.1521-1527, Oct.2001.
- [3] Zhang and X. Wu, "Image interpolation via directional filtering and data fusion," *IEEE Trans. Image Process.*, vol.15, no.8, pp.2226-2238, Aug.2006.
- [4] Takeda, H., S. Farsiu, and P. Milanfar, "Kernel Regression for Image Processing and Reconstruction," *IEEE Trans. Image Process.*, vol.16, No.2, pp.349-366, February 2007.
- [5] X. Zhang, X. Wu, "Image Interpolation by Adaptive 2-D Autoregressive Modeling and Soft-Decision Estimation," *IEEE Trans. Image Process.*, vol.17, no.6, pp.887-896, June 2008.
- [6] R. T. T. Hastie and J. Friedman. *The Elements of Statistical Learning: Data Mining, Inference, and Prediction*. Springer-Verlag, 2001.
- [7] M. Belkin, P. Niyogi, and V. Sindhwani, "Manifold regularization: A geometric framework for learning from examples," *J. Mach. Learn. Res.*, vol. 7, pp. 2399-2434, 2006.
- [8] C. Tomasi and R. Manduchi, "Bilateral filtering for gray and color images," in *Proceedings of the IEEE International Conference on Computer Vision*, pages 839-846, 1998.
- [9] A. Buades, B. Coll, and J. M. Morel, "A review of image denoising algorithms, with a new one," *Multiscale Modeling Simulation*, vol. 4,no. 2, pp. 490-530, 2005.